How to Perform Resolution & Noise Analysis on Virtual Microstructures using DREAM.3D

All of the virtual microstructural analysis performed throughout this dissertation used various versions of DREAM.3D [10] (dream3d.bluequartz.net), which has been under constant development for the duration of the research. The link above can be used to download any current or historical version of the software. Note that the analysis for the journal publication associated with section 3.1 in the dissertation [99] was performed using version 2, while the more recent case studies on Inconel 100 and Ti-6Al-4V β grains were completed with version 5. Version 6, the most current version set for release this year, was used for the resolution and noise + cleanup analysis, and it is this most recent version employed herein.

Outlined below is a process by which anyone can perform similar analyses to those presented in this dissertation using DREAM.3D and MATLAB™, including investigating the effects of both resolution and noise (boundary and/or random) by comparing geometric similarity of PDFs and the percentage error in mean values of PDFs for the following microstructural distributions: grain size (equivalent sphere diameter), grain shape (aspect ratio *b/a* and *c/a*), and the number-of-nearest neighbor grains. Although the code provided operates within the parameters listed above, it can be easily modified to include additional types of microstructures, sources of error, microstructural parameters, statistical analyses, etc. Much of this modification can be completed through use of these files and/or the DREAM.3D graphical user interface (GUI). Screenshots included in this procedure were taken on a machine using a Windows 7 64-bit operating system, but DREAM.3D is compatible with Windows, Apple, and Linux platforms. Lastly, please note that some code modification will be required, as hard-coded file paths are based on my file structures, and some of the hard-coded character counters in the MATLAB™ files PipelineCreator.m and PipelineRunner.m will need to be modified, as

will the file path hard-coded in ResAndNoise.m. The file paths in Phantom_Build_Stats.json

and DownSample.json can be easily updated via the DREAM.3D GUI.

Feel free to contact the author if you have any questions or comments regarding the use of

*this analysis code. ~ *Corresponding author.* **Email Address: greg.loughnane@gmail.com***

1. <u>*Software Download and File Construction*</u>: Download Version 6 of DREAM.3D and create

   the files listed below in the appropriate format based on the raw code provided in Appendix

   B.

   1. Phantom_Build_Stats.json

   2. Downsample.json

   3. PipelineCreator.m

   4. ScanPrintLine.m

   5. PipelineRunner.m

   6. GetCSVs.m

   7. ComputeGrainStatistics.m

   8. ResAndNoise.m

2. <u>*Create Statistical Input Size Distribution*</u>: After downloading DREAM.3D and copying the

   MATLAB files provided in Appendix B, navigate to the new folder and open

   StatsGenerator.exe.

	3/1/...	Application	1,457 KB	DREAM3D.exe
	3/1/...	Application	122 KB	PipelineRunner.exe
	3/1/...	Application	671 KB	PluginMaker.exe
	3/1/...	Application	2,847 KB	StatsGenerator.exe
	3/1/...	Application e...	5,215 KB	DREAM3DLib.dll
	3/1/...	Application e...	3,293 KB	DREAM3DWidgetsLib.dll

Choose the microstructure you wish to model by defining an input distribution for grain size. The user can choose to define additional distributions for shape, neighbors, and grain orientation, but based on the grain size input and the Preset Statistical Model, the other distributions will be assigned automatically when "Create Data" is clicked. These other distributions are generated based on microstructural correlations known to exist for the type of Preset Statistic Model (see Ref [87] for an example of these correlations).

After creating the input distributions, save the file in the main DREAM.3D folder.
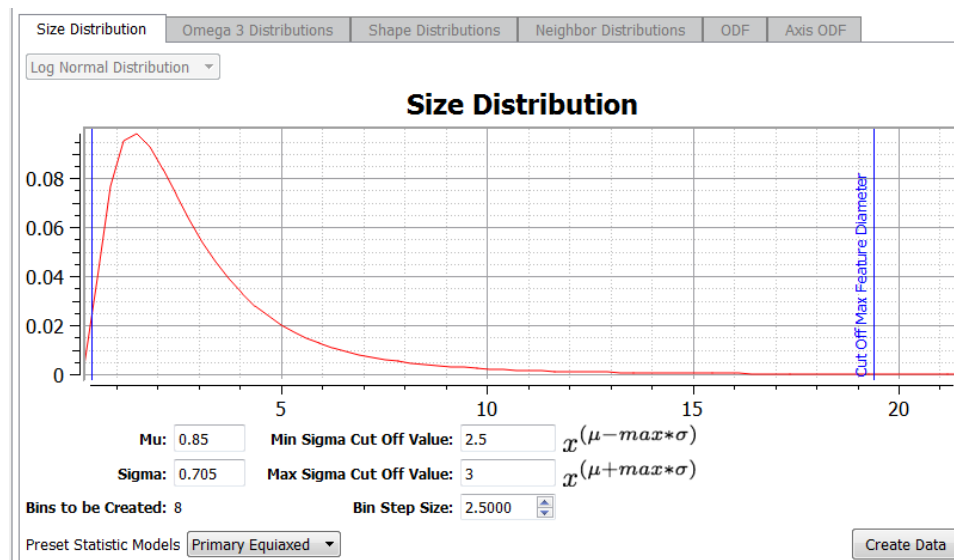
3. *Modify Phantom_Build_Stats.json & Downsample.json via DREAM.3D GUI:* Open DREAM3D.exe and then open Phantom_Build_Stats.json. You will likely be prompted to replace the input statistics file with the one that you just generated. Go through each filter and make sure that there are no remaining red filters like the one shown below. Red denotes

an error that will prohibit DREAM.3D from running the pipeline. Update all file names and file paths so that they are associated with your file structures.
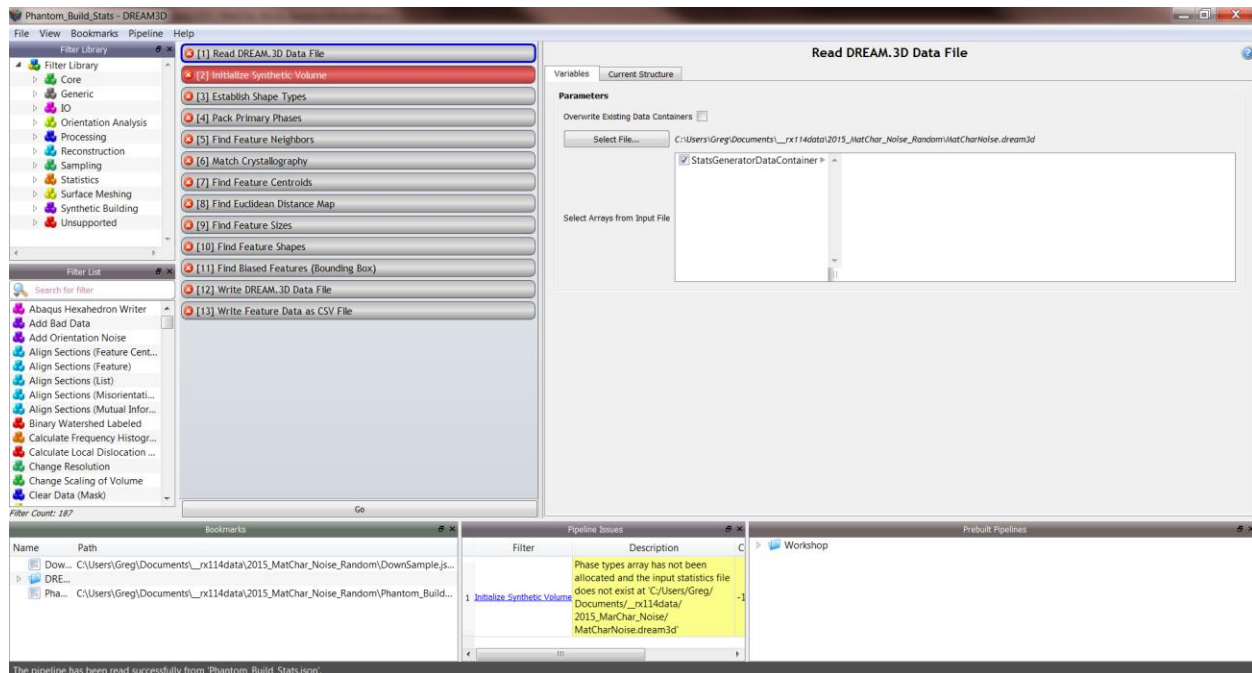

Go through the same procedure with the DownSample.json file. Note that you can also run a single experiment using just these input files and the DREAM.3D GUI. If this is your first time using DREAM.3D this is a good idea, because you can simply click "Go" in the GUI, perform a single phantom build and down-sampling, and then visualize your new microstructures.

4. *Download the Latest Version of Paraview to View the Microstructures You Just Created:*
   Navigate your web browser to Paraview.org and download the latest version. This software is used to visualize the microstructures that are created with DREAM.3D.

    Once downloaded, open the software, navigate to the folder where you are saving your created files (this should be the same DREAM.3D folder that StatsGenerator.exe and DREAM3D.exe are in), and open the phantom reference volume generated from

Phantom_Build_Stats.json in DREAM.3D (.xdmf file type). You should see something like this once the file loads:
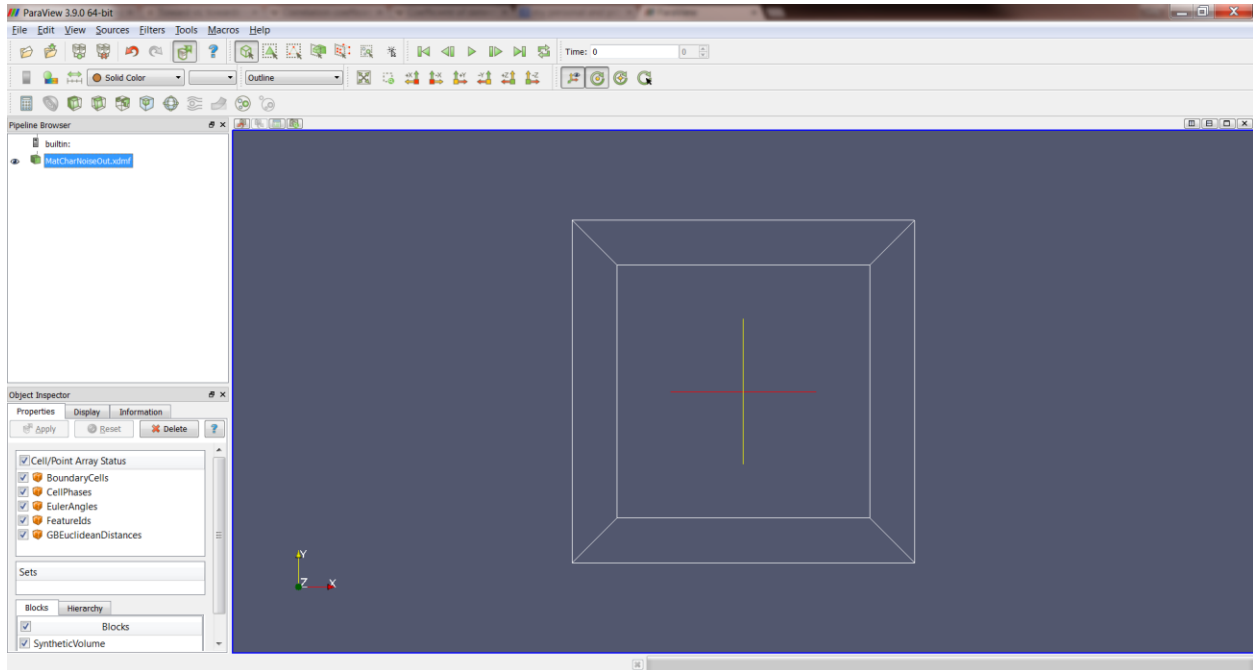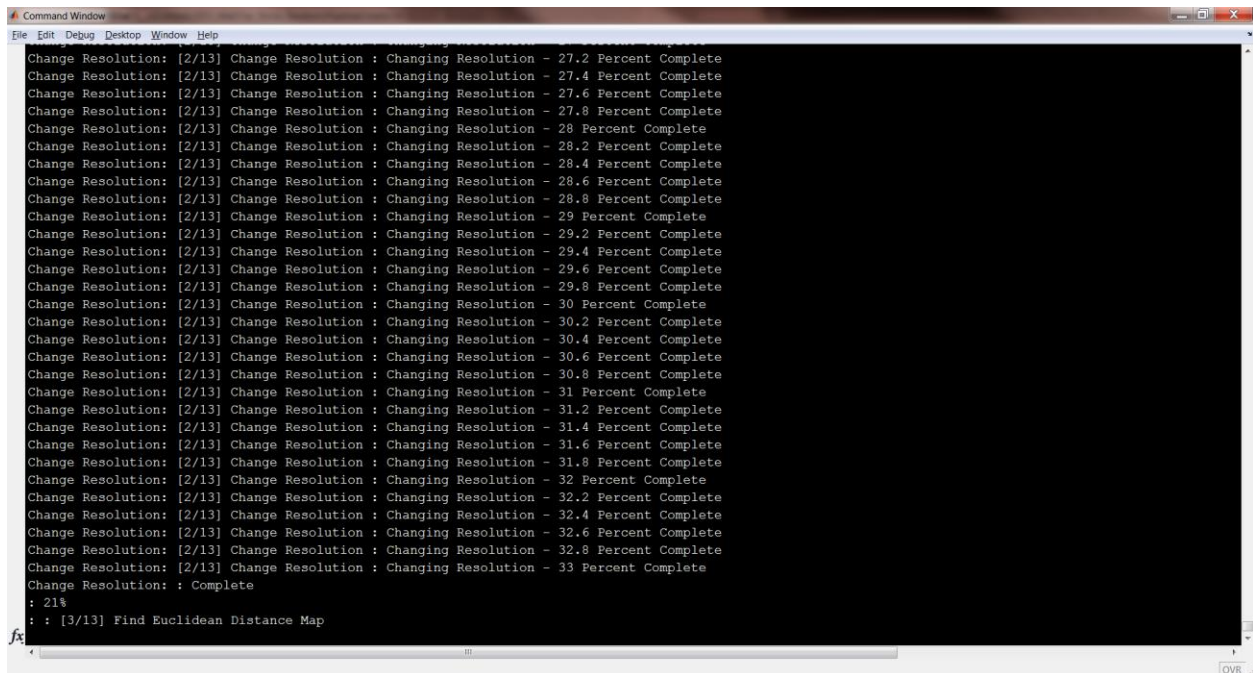

From the drop down menu that reads "Outline," select "Surface". Then, from the drop down menu that reads "Solid Color" select "FeatureIds". You should now be able to see your microstructure and use the mouse to move it as you would with any typical 3D modeling software.
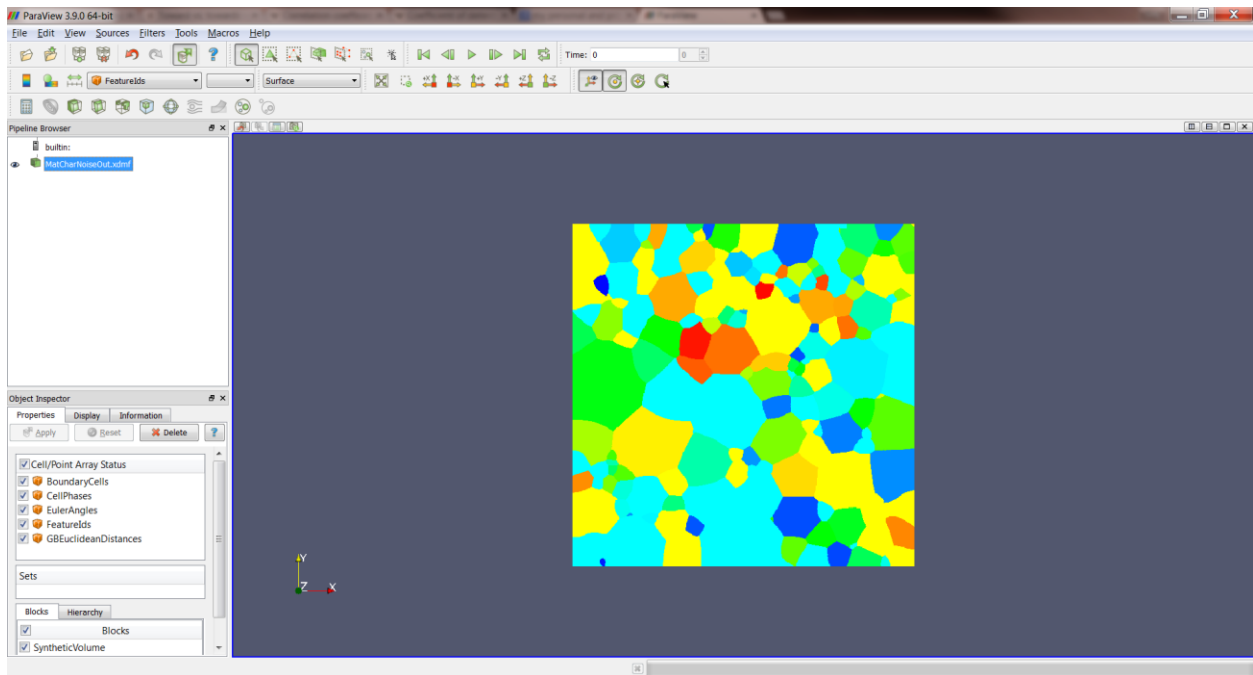
To compare the two visually, feel free to go through these steps with the down-sampled volume as well.

5. *Modify PipelineCreator.m for Your File Structure:* Count the number of characters in the file path string associated with the .dream3d and .csv output files that you created from DownSample.json. Update PipelineCreator.m to reflect these changes in lines 38 and 46, respectively.

6. *Modify ResAndNoise.m for Your Experiment:* Open ResAndNoise.m and modify the file directory, the resolutions desired for analysis, the noise levels to be investigated, the average grains size, and the instantiation number (which represents the number of times you wish to perform each experiment). Assuming that you will only analyze grain size, aspect ratios, and number-of-nearest neighbors as a first cut, there are just a few modifications that you still must make to the ComputeGrainStatistics.m file, which are noted at the top of the code in Appendix B.
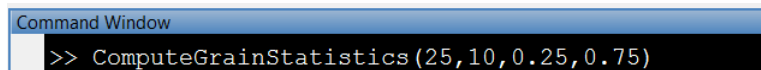
7. *Run ResAndNoise.m:* Try to run the ResAndNoise.m file. If it is successful, you should see the command window in MATLAB™ doing something like this:

If so, congratulations! If not, then it's time to debug the code. Check that all of your files are located in the DREAM.3D folder that you originally downloaded, check file paths, etc.

8. *Compute Statistics from Down-Sampled Volumes:* Once you have all of your statistical data following the simulations, run ComputeGrainStatistics.m from the command window using, for example, the following input parameters:

Select the reference volume statistics file for comparison first:
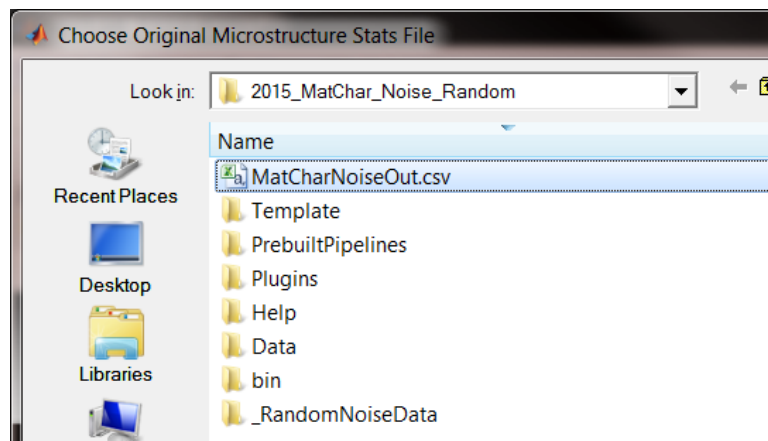
Then choose the down-sampled volume statistics file(s):
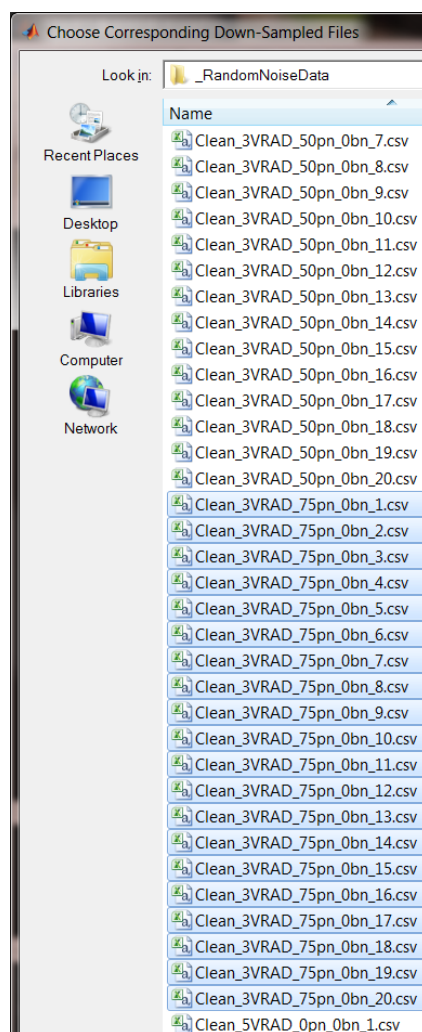
You will be prompted to name the output file, and when you do results there will be some select results written to the command window. You can ignore these, as they are saved along with other data automatically in .csv file format.

```
Command Window
    >> ComputeGrainStatistics(25,10,0.25,0.75)
fx  What do you want to call these results? :
```

9. *View Final Statistics Computed between Reference and Down-Sampled Volumes*: Navigate to the files you just created and open "YourFileName_MBCandPercErrMean.csv". It will appear without descriptive text, however the results correspond to the data shown below, where the numbers in column C correspond to the 95% confidence interval on the answers reported in column B.

Type	Size	Name
File folder		_RandomNoiseData
File folder		bin
File folder		Data
File folder		Help
File folder		Plugins
File folder		PrebuiltPipelines
File folder		Template
Microsoft Exc...	6 KB	3VRAD_0RN_DistData.csv
Microsoft Exc...	1 KB	3VRAD_0RN_MBCandPercErrMeanData.csv
Microsoft Exc...	6 KB	3VRAD_10RN_DistData.csv
Microsoft Exc...	1 KB	3VRAD_10RN_MBCandPercErrMeanData.csv
Microsoft Exc...	7 KB	3VRAD_25RN_DistData.csv
Microsoft Exc...	1 KB	3VRAD_25RN_MBCandPercErrMeanData.csv
Microsoft Exc...	7 KB	3VRAD_50RN_DistData.csv
Microsoft Exc...	1 KB	3VRAD_50RN_MBCandPercErrMeanData.csv
Microsoft Exc...	6 KB	3VRAD_75RN_DistData.csv
Microsoft Exc...	1 KB	3VRAD_75RN_MBCandPercErrMeanData.csv

	A	B	C
1			
2	MBC, ESD	0.29454	0.004274
3	MBC, b/a	0.42878	0.003163
4	MBC, c/a	0.48655	0.002974
5	MBC, NNN	0.13908	0.004856
6		########	########
7	Low Quantile MBC, ESD	0.5617	0.002088
8	Low Quantile MBC, b/a	0.35336	0.005442
9	Low Quantile MBC, c/a	0.37728	0.003042
10	Low Quantile MBC, NNN	0.082518	0.00414
11		########	########
12	High Quantile MBC, ESD	0.06453	0.005014
13	High Quantile MBC, b/a	0.41474	0.004356
14	High Quantile MBC, c/a	0.22027	0.009691
15	High Quantile MBC, NNN	0.08564	0.001874
16		########	########
17	Percent Error in Mean, ESD	21.061	0.38266
18	Percent Error in Mean, b/a	-12.855	0.22519
19	Percent Error in Mean, c/a	-22.326	0.18256
20	Percent Error in Mean, NNN	-0.31048	0.25767
21			

Next open "YourFileName_DistData.csv". These are the collective distributions, with corresponding error bars for each bin and the percent difference in down-sampled

distribution bins relative to the reference volume. ESD is shown first, followed by number-of-nearest neighbors, aspect ratio b/a, and aspect ratio c/a.

	Bins	Reference Distribution	Down-Sampled Distribution	95% Confidence Interval For Each Distribution Bin	Percent Difference From Reference Distribution For Each Bin
ESD	0.25	0.010681	0	0	1.0681
	0.75	0.076101	0.0032414	0.00079252	7.286
	1.25	0.17223	0.020782	0.0019551	15.145
	1.75	0.17824	0.14369	0.0044843	3.455
	2.25	0.13818	0.20655	0.0065342	6.8369
	2.75	0.098798	0.15694	0.0047989	5.8141
	3.25	0.074099	0.11793	0.0039143	4.3828
	3.75	0.061415	0.085595	0.0034923	2.418
	4.25	0.048732	0.061447	0.0025315	1.2716
	4.75	0.026702	0.045723	0.0019991	1.902
	5.25	0.024032	0.040726	0.0024344	1.6694
	5.75	0.016021	0.029464	0.0018614	1.3442
	6.25	0.012684	0.022574	0.0013139	0.98908
	6.75	0.015354	0.011328	0.0011483	0.40262
	7.25	0.011348	0.011386	0.0008595	0.0037177
	7.75	0.010681	0.013535	0.0011005	0.28536
	8.25	0.0040053	0.0059755	0.00081244	0.19702
	8.75	0.0040053	0.0020409	0.0005303	0.19645
	9.25	0.0040053	0.0040396	0.00066763	0.0034281
	9.75	0.0033378	0.0061608	0.00074428	0.2823
	10.25	0.0020027	0.0037292	0.00043004	0.17266
	10.75	0.0026702	0.0011974	0.00036989	0.14728
	11.25	0.0020027	0.002101	0.00020018	0.0098306
	11.75	0	0.0011911	0.00032108	0.11911
	12.25	0.00066756	0.0014638	0.00033607	0.079628
	12.75	0.00066756	0.0003496	0.00025679	0.031795
	13.25	0.00066756	0.0008414	0.00023362	0.017385

3VRAD_75RN_DistData

Ready

	Bins	Reference Distribution	Down-Sampled Distribution	95% Confidence Interval For Each Distribution Bin	Percent Difference From Reference Distribution For Each Bin
NNN	########	1.00E+100	1.00E+100	1.00E+100	1.00E+100
	0	0	0	0	0
	0.04	0	0	0	0
	0.08	0	0	0	0
	0.12	0	0	0	0
	0.16	0	0	0	0
	0.2	0	0.0005639	0.00040086	0.05639
	0.24	0	5.77E-05	0.0001207	0.005767
	0.28	0	0.0054935	0.001071	0.54935
	0.32	0	0.00039318	0.00030725	0.039318
	0.36	0	0.0011381	0.00054199	0.11381
	0.4	0	0.0040694	0.0011494	0.40694
	0.44	0	0.028574	0.0023598	2.8574
	0.48	0.0013351	0.018635	0.0023538	1.7299
	0.52	0.00066756	0.020702	0.0021403	2.0034
	0.56	0.00066756	0.030931	0.0023675	3.0264
	0.6	0.0033378	0.057215	0.0039917	5.3877
	0.64	0.0080107	0.12678	0.0042849	11.877
	0.68	0.014686	0.06884	0.0043582	5.4153
	0.72	0.042724	0.09194	0.0045309	4.9216
	0.76	0.076769	0.1184	0.0050311	4.1629
	0.8	0.11415	0.096868	0.0045773	1.7284
	0.84	0.17423	0.091522	0.0038931	8.271
	0.88	0.24032	0.092118	0.0036156	14.82
	0.92	0.21762	0.073208	0.002823	14.442
	0.96	0.10414	0.02848	0.0029358	7.5659
	1	0.0013351	0.044076	0.0038258	4.274

3VRAD_75RN_DistData

Ready

You have officially completed this tutorial. Have fun plotting the data and identifying trends to inform future microstructural characterization!

Cheers,

Greg Loughnane

References

1   DeHoff, R.T., "Quantitative serial sectioning analysis: preview," *Journal of Microscopy*, Vol. 131, Issue 3, September 1983, pp. 259–263.

2   Russ, J.C., DeHoff, R.T. (1986), *Practical stereology*: Plenum Press.

3   Alkemper, J., Voorhees P.W., "Quantitative serial sectioning analysis," *Journal of Microscopy*, Vol. 201, Issue 3, March 2001, pp. 388–394.

4   Spowart, J.E., Mullens, H.M., and Puchala, B.T., "Collecting and analyzing microstructures in three dimensions: a fully automated approach," *Journal of Materials*, Vol. 55, Issue 10, pp. 35–37.

5   Adachi, Y., "Fully-automated Serial Sectioning 3D Microscopy," in *The International Conference on Nano Materials Synthesis and Characterization Proceedings*, Malaysia, July 2011.

6   Uchic, M., Groeber, M., Shah, M., Callahan, P., Shiveley, A., Scott, M., Chapman, M. and Spowart, J., "An Automated Multi-Modal Serial Sectioning System for Characterization of Grain-Scale Microstructures in Engineering Materials," *in 1st International Conference on 3D Materials Science*, Seven Springs, PA, July 2012, pp. 195-202.

7   Uchic, M.D., Groeber, M.A., and Rollet, A.D., "Automated Serial Sectioning Methods for Rapid Collection of 3-D Microstructure Data," *Journal of Materials*, Vol. 63, Issue 3, 2011, pp. 25-29.

8   Uchic, M.D., "Serial Sectioning Methods for Generating 3D Characterization Data of Grain- and Precipitate-Scale Microstructures" in *Computational Methods for Microstructure-Property Relationships*, S. Ghosh and D. Dimiduk (co-editors), pp. 31-52, Springer NY, December 2010.

9   Groeber, M.A., "Digital Representation of Materials Grain Structure" in *Computational Methods for Microstructure-Property Relationships*, S. Ghosh and D. Dimiduk (co-editors), pp. 53-97, Springer NY, December 2010.

10   Groeber, M.A., Jackson, M.A., "DREAM.3D: A Digital Representation Environment for the Analysis of Mirostructure in 3D," *Integrating Materials and Manufacturing Innovation*, Vol. 3, Issue 5, 2014.

11   Materials Genome Initiative for Global Competitiveness, June 2011.

12   Allison, J., "Integrated Computational Materials Engineering: A Perspective on Progress and Future Steps," *Journal of Materials*, Vol. 63, Issue 4, April 2011, pp. 15-18.

13   Christodoulou, J., "Dynamic 3D Digital Structure: Program Overview," *Journal of Materials*, Vol. 61, Issue 10, 2009, p. 21.

14   Dimiduk, D., "Microstructure-Property-Design Relationships in the Simulation Era An Introduction" in *Computational Methods for Microstructure-Property Relationships*, S. Ghosh and D. Dimiduk (co-editors), pp.1-28, Springer NY, December 2010.

15   Vander Voort, G.F. (2004). *ASM Handbook, Volume 09 - Metallography and Microstructures*: ASM International.

16   Larson, B.C., Yang, W., Ice, G.E., Budai, J.D., and Tischler, J.Z., "Three-dimensional X-ray structural microscopy with submicrometre resolution," *Nature*, Vol. 415, 2002, pp. 887-890.

17   Brandon, D., Kaplan, W.D (2008). *Microstructural Characterization of Materials*: Wiley.

18   Groeber, M.A., Haley, B.K., Uchic, M.D., Dimiduk, D.M., and Ghosh, S., "3D reconstruction and characterization of polycrystalline microstructures using a FIB-SEM system," *Materials Characterization*, Vol. 57, 2006, pp. 259-273.

19   Hara T., Tsuchiya K., Tsuzaki K., Man X., Asahata T., and Uemoto A., "Application of orthogonally arranged FIB-SEM for precise microstructure analysis of materials", *Journal of Alloys and Compounds* Vol. 577, Supplement 1, 2013, pp. 717–721.

20   Hara, T., "Recent improvement of a FIB-SEM serial-sectioning method for precise 3D image reconstruction – application of the orthogonally-arranged FIB-SEM," *Microscopy* (Tokyo), Vol. 63, Supplement 1, 2014.

21   Hara T., "3D Microstructure observation of materials by means of FIB-SEM serial sectioning," *KENBIKYO*, Vol. 49, Issue 1, 2014, pp. 53–58.

22   Dillon, S. J., and Rohrer, G. S., "Characterization of the Grain-Boundary Character and Energy Distributions of Yttria Using Automated Serial Sectioning and EBSD in the FIB," *Journal of the American Ceramic Society*, Vol. 92, Issue 7, July 2009, pp. 1580-1585.

23   Konrad J, Zaefferer S, and Raabe D., "Investigation of orientation gradients around a hard Laves particle in a warm-rolled Fe3Al-based alloy using a 3D EBSD-FIB technique," *Acta Materialia*, Vol. 54, Issue 5, March 2006, pp. 1369–1380.

24   Bansal, R.K., Kubis, A., Hull, R., and Fitz-Gerald, J.M., "High-resolution three-dimensional reconstruction: A combined scanning electron microscope and focused ion beam approach," *Journal of Vacuum Science Technology*, Vol. 24, Issue 3, April 2006, pp. 554-561.

25   Uchic, M.D., Groeber, M.A., Dimiduk, D.M., and Simmons, J.P., "3D microstructural characterization of nickel superalloys via serial-sectioning using a dual beam FIB-SEM," *Scripta Materialia*, Vol. 55, Issue 1, July 2006, pp. 23-38.

26   Rowenhorst, D. J., and Spanos, G., "Crystallographic and Morphological Analysis by Combining EBSD and Serial Sectioning," *Microscopy and Microanalysis*, Vol. 13, Supplement S02, August 2007, pp. 934-935.

27   Tiley, J.S., Shiveley, A.R., Pilchak, A.L., Shade, P.A., and Groeber, M.A., "3D Reconstruction of prior β grains in friction stir-processed Ti-6Al-4V," *Journal of Microscopy*, Vol. 255, Issue 2, 2014, pp. 71-77.

28   Schwarzer, R.A., Field, D.P, Adams, B.L., Kumar, M., and Schwartz, A.J., "Present State of Electron Backscatter Diffraction and Prospective Developments," *in Electron Backscatter Diffraction in Materials Science,* ed. Schwartz, A.J., Kumar, M., Adams, B.L., and Field, D.P., Springer NY, 2009.

29   Cooper, D., Turinsky, A., Sensen, C., and Hallgrimsson, B., "Effect of voxel size on 3D micro-CT analysis of cortical bone density," *Calcified Tissue International*, Vol. 80, Issue 3, March 2007, pp. 211-219.

30   Lewis, A.C., Qidwai, S.M., Jackson, M., Geltmacher, A.B., "Strategies for Integration of 3D Experimental Data with Modeling and Simulation," *Journal of Materials*, Vol. 63, Issue 3, 2011, pp. 35-39.

31   Rollett, A.D., Lebensohn, R.A., Groeber, M., Choi, Y., Li, J., and Rohrer, G.S., "Stress hot spots in viscoplastic deformation of polycrystals," *Modeling and Simulation in Materials Science and Engineering*, Vol. 18, Issue 7, October 2010.

32   Brockman, R.A., Pilchak, A.L., Porter, J., and John, R., "Estimation of grain boundary diffusivitiy in near-α titanium polycrystals," *Scripta Materialia*, Vol. 65, Issue 6, September 2011, pp. 513-515.

33   Uetsuji, Y, Kimura, S., Kuramae, H., Tscuchiya, K.,and Kamlah, M., "Multiscale finite element simulations of piezoelectric materials based on two- and three-dimensional electron backscatter diffraction-measured microstructures," *Journal of Intelligent Material Systems and Structures*, Vol. 23, Issue 5, pp. 563-573.

34   Donegan, S.P., Tucker, J.C., Rollett, A.D., Barmak, K., and Groeber, M., "Extreme value analysis of tail departure from log-normality in experimental and simulated grain size distributions," *Acta Materialia*, Vol. 61, Issue 15, September 2013, pp. 5595-5604.

35   Sintay, S.D. (2010). *Statistical microstructure generation and 3D microstructure geometry extraction* (Electronic dissertation). Retrieved from ProQuest Dissertations and Theses (Accession Order No. UMI 3421737).

36   Groeber, M. (2007). *Development of an automated characterization-representation framework for the modeling of polycrystalline materials in 3D* (Electronic Dissertation). Retrieved from https://etd.ohiolink.edu.

37   Cho, J., "Microstructure Predictability by Voronoi Diagram," *Future Information Technology, Application, and Service*, Vol. 164, 2012, pp. 615-619.

38   Spettl, A., Werz., T, Krill, C. E., and Schmidt, V., "Parametric representation of 3D grain ensembles in polycrystalline microstructures," *Journal of Statistical Physics*, Vol. 154, Issue 4, February 2014, pp. 913-928.

39   McDowell, D.L., Ghosh, S., and Kalidindi, S.R., "Representation and Computational Structure-Property Relations of Random Media," *Journal of Materials*, Vol. 63, Issue 3, March 2011, pp. 45-51.

40   The Minerals, Metals & Materials Society. (2013). Integrated Computational Materials Engineering (ICME): Implementing ICME in the Aerospace, Automotive, and Maritime Industries. Retrieved from http://www.tms.org/icmestudy.

41   The Minerals, Metals & Materials Society. (2015). Modeling Across Scales: A Roadmapping Study for Connecting Materials Models and Simulations Across Length and Time Scales. Retrieved from http://www.tms.org/multiscalestudy.

42   Patterson, B.M., Escobedo-Diaz, J.P., Dennis-Koller, D., and Cerreta, E., "Dimensional Quantification of Embedded Voids or Objects in Three Dimensions Using X-Ray Tomography," *Microanalysis*, Vol. 18, Issue 2, 2012, pp. 390-398.

43   Sintay, S.D., and Rollet, A.D., "Testing the accuracy of microstructure reconstruction in 3D using phantoms," *Modelling and Simulation in Materials Science and Engineering*, Vol. 18, Issue 7, October 2012, 18 pages.

44   Tiwari, S., and Tewari, A., "Inherent limitations of bitmap discretization in quantitative microstructural analysis," *Materials Characterization*, Vol. 61, Issue 5, May, 2010, pp. 493-501.

45   Gibson, D., Rosen, W., and Stucker, B. (2010), *Additive Manufacturing Technologies*: Springer.

46   Gausemeier, J., Echterhoff, N., Kokoschka, M., and Wall, M., "Thinking ahead the Future of Additive Manufacturing – Analysis of Promising Industries," *Heinz Nixdorf Institute, University of Paderborn*, 2011.

47   Taminger, K.M., and Hafley, R.A., "Electron Beam Freeform Fabrication: a rapid metal deposition process," in *3rd Annual Automotive Composites Conference Proceedings*, 2003.

48   Taminger, K.M., and Hafley, R.A., "Electron Beam Freeform Fabrication for Cost Effective Near-Net Shape Manufacturing," *NATO/RTOAVT-139 Specialist' Meeting on Cost Effective Manufacture via Net Shape Processing*, Amsterdam, Netherlands, 2006.

49   Beuth, J., Fox, J., Gockel, J., Montgomery, C., Yang, R., Qiao, H., Soylemez, E., Reeseewatt, P., Anvari, A., Narra, S., and Klingbeil, N., "Process Mapping Across Multiple Direct Metal Additive Manufacturing Processes," in *Solid Freeform Fabrication Proceedings*, Austin, 2013, pp. 655-665.

50   Klingbeil, N.W., Zinn, J.W., and Beuth, J.L., "Measurement of residual stresses in parts created by shape deposition manufacturing," in *Solid Freeform Fabrication Proceedings*, Austin, 1997, pp. 125-132.

51   Klingbeil, N.W., Beuth, J.L, Chin, R.K., and Amon, C.H., "Measurement and modeling of residual stress-induced warping in direct metal deposition processes," in *Solid Freeform Fabrication Proceedings*, Austin, 1998, pp. 367-374.

52   Ong, R., Beuth, J.L., and Weiss, L.E., "Residual stress control issues for thermal deposition of polymers in SFF processes," in *Solid Freeform Fabrication Proceedings*, Austin, 2000, pp. 209-218.

53 Klingbeil, N.W., Beuth, J.L, Chin, R.K., and Amon, C.H., "Residual stress-induced warping in direct metal solid freeform fabrication," *International Journal of Mechanical Science*s, Vol. 44, 2002, pp. 57-77.

54 Vasinonta, A., Beuth, J.L., and. Griffith, M., "Process maps for predicting residual stress and melt pool size in the laser-based fabrication of thin-walled structures," *Journal of Manufacturing Science and Engineering*, Vol. 129, Issue 1, 2007 pp. 101-109.

55 Vasinonta, A., Beuth, J.L., and Ong, R., "Melt pool size control in thin-walled and bulky parts via process maps," in *Solid Freeform Fabrication Proceedings*, Austin, 2001, pp. 432-440.

56 Vasinonta, A., Beuth, J.L., and. Griffith, M., "A Process Map for Consistent Build Conditions in the Solid Freeform Fabrication of Thin-Walled Structures," *ASME Journal of Manufacturing Science and Engineering*, Vol. 123, Issue 4, 2001, pp. 615-622.

57 Vasinonta, A., Beuth, J.L., and. Griffith, M., "Process Maps for Laser Deposition of Thin-Walled Structures," in *Solid Freeform Fabrication Proceedings*, Austin, 1999, pp. 383-391.

58 Beuth, J.L., and Klingbeil, N.W., "The Role of Process Variables in Laser-Based Direct Metal Solid Freeform Fabrication," *Journal of Materials*, Vol. 53, Issue 9, September 2001, pp. 36-39.

59 Vasinonta, A. (2002) *Process Maps for Melt Pool Size and Residual Stress in Laser-Based Solid Freeform Fabrication* (Electronic dissertation). Retrieved from ProQuest Dissertations and Theses.

60 Klingbeil, N.W., Brown, C., Bontha, S., Kobryn, P., and Fraser, H., "Prediction of Microstructure in Laser Deposition of Titanium Alloys," in *Solid Freeform Fabrication Proceedings*, Austin, 2002, pp. 142-149.

61 Klingbeil, N.W., Bontha, S., Brown, C.J., Gaddam, D.R., Kobryn, P.A., Fraser, H.L., Sears, J.W., "Effects of Process Variables and Size Scale on Solidification Microstructure in Laser-Based Solid Freeform Fabrication of Ti-6Al-4V," in S*olid Freeform Fabrication Proceedings*, Austin, 2004, pp. 92-103.

62 Bontha, S. and Klingbeil, N.W., "Thermal Process Maps for Controlling Microstructure in Laser-Based Solid Freeform Fabrication," *Solid Freeform Fabrication Proceedings*, Austin, 2003, pp. 219-226.

63 Bontha, S., Klingbeil, N.W., Kobryn, P., and Fraser, H.L., "Effects of Process Variables and Size Scale on Solidification Microstructure in Beam-Based Fabrication of Bulky 3D Structures," *Materials Science and Engineering A*, Vol. 513-514, 2009, pp. 311-318.

64 Bontha, S., Klingbeil, N.W, Kobryn, P., and Fraser, H.L., "Thermal Process Maps for Predicting Solidification Microstructure in Laser Fabrication of Thin Wall Structures," *Journal of Materials Processing Technology*, Vol. 178, 2006, pp. 135-142.

65 Bontha, S. (2006) *The Effect of Process Variables on Microstructure in Laser Deposited Materials* (Electronic Dissertation). Retrieved from https://etd.ohiolink.edu.

66 Davis, J., Klingbeil, N., and Bontha, S., "Effect of Free-Edges on Melt Pool Geometry and Solidification Microstructure in Beam-Based Fabrication of Bulky 3-D Structures," in *Solid Freeform Fabrication Proceedings*, Austin, 2010, pp. 230-241.

67   Davis, J., Klingbeil, N., and Bontha, S., "Effect of Free-Edges on Melt Pool Geometry and Solidification in Beam-Based Fabrication of Thin-Wall Structures," in *Solid Freeform Fabrication Proceedings*, Austin, 2009, pp. 320-331.

68   Beuth, J.L., "Methods for Determining Process Variable Combinations Yielding Constant Melt Pool Geometry for Single Bead Deposits in Direct Digital Manufacturing," *Materials Science and Technology*, Vol. 31, Issue 8, June 2015, pp. 912-916.

69   Gockel, J., and Beuth, J., "Understanding Ti-6Al-4V Microstructure Control in Additive Manufacturing via Process Maps," in *Solid Freeform Fabrication Proceedings*, Austin, 2013, pp. 666-674.

70   Griffith, M.L., Keicher, D.M., Atwood, C.L., Romero, J.A., Smugeresky, J.E., Harwell, L.D., and Greene, D.L., "Free Form Fabrication of Metallic Components Using Laser Engineered Net Shaping (LENS™)," in *Solid Freeform Fabrication Proceedings,* Austin, 1996, pp. 125-132.

71   Purtonen, T., Kalliosaari, A., and Salminen, A., "Monitoring and adaptive control of laser processes," *Physics Procedia*, Vol. 56, 2014, pp. 1218-1231.

72   Reutzel, E.W., Nassar, A.R., "A survey of sensing and control systems for machine and process monitoring of directed-energy, metal-based additive manufacturing," *Rapid Prototyping Journal*, Vol. 21, Issue 2, 2015, pp.159-167.

73   Griffith, M.L., Schlienger, M.E., Harwell, L.D., Oliver, M.S., Baldwin, M.D., Ensz, M.T., Essien, M., Brooks, J., Robino, C.V., Smugeresky, J., Hofmeister, W.H., Wert, M.J., and Nelson, D.V., "Understanding thermal behavior in the LENS process," *Materials & Design*, Vol. 20, Issue 2, June 1999, pp. 107–113.

74   Hofmeister, W., Knorovsky, G.A., and MacCallum, D.O., "Video monitoring and control of the LENS process," *AWS 9th International Conference on Computer Technology in Welding Proceedings*, 1999, pp. 417-424.

75   Hofmeister, W., Griffith, M., Ensz, M., and Smugeresky, J., "Solidification in direct metal deposition by LENS processing," *Journal of Materials*, Vol. 53, Issue 9, 2001, pp. 30–34.

76   Wu, X., Liang, J., Mei, J., Mitchell, C., Goodwin, P., and Voice, W., "Microstructures of laser-deposited Ti–6Al–4V," *Materials & Design*, Vol. 25, Issue 2, 2004, pp. 137–144.

77   Brandl, E., Leyens, C., and Palm, F., "Mechanical properties of additive manufactured Ti–6Al–4V using wire and powder based processes," *Materials Science and Engineering*, Vol. 26, Issue 1, 2011, 10 pages.

78   Brandl, E., Michailov, V., Viehweger, B., and Leyens, C., "Deposition of Ti–6Al–4V using laser and wire, part I: Microstructural properties of single beads," *Surface and Coatings Technology*, Vol. 206, Issue 6, December 2011, pp. 1120–1129.

79   Kelly, S.M., and Kampe, S.L., "Microstructural evolution in laser-deposited multilayer Ti-6Al-4V builds: Part I. Microstructural characterization," *Metallurgical and Materials Transactions A*, Vol. 35, Issue 6, June 2004, pp. 1861-1867.

80   Kelly, S.M., and Kampe, S.L., "Microstructural evolution in laser-deposited multilayer Ti-6Al-4V builds: Part II. Thermal Modeling," *Metallurgical and Materials Transactions A*, Vol. 35, Issue 6, June 2004, pp. 1869-1879.

81   Donachie, M. J. (2000) *Titanium: A Technical Guide*: ASM International.

82   Burgers, W.G., "On the process of transition of the cubic-body-centered modification into the hexagonal-close-packed modification of zirconium," *Physica 1*, Vol. 1, May 1934, pp. 61-86.

83   Sargent, G.A., Kinsel, K.T., Pilchak, A.L, Salem, A.A., and Semiatin, S.L., "Variant Selection During Cooling after Beta Annealing of Ti-6Al-4V Ingot Material," *Metallurgical and Materials Transactions A*, Vol. 43, Issue 10, pp. 3570-3585.

84   Kelly, S.M. (2004) *Thermal and Microstructure Modeling of Metal Deposition Processes with Application to Ti-6Al-4V* (Electronic Dissertation). (etd-11242004-211009).

85   Collins, P.C., Welk, B., Searles, T., Tiley, J., Russ, J.C., and Fraser, H.L., "Development of methods for the quantification of microstructurl features in α+β-processed α/β titanium alloys," *Materials Science and Engineering A*, Vol. 508, May 2009, pp. 174-182.

86   Neal, F.B., and Russ, J.C. (2012). *Measuring Shape*: CRC Press.

87   Groeber, M., Ghosh, S., Uchic, M.D., and Dimiduk, D.M., "A framework for automated analysis and simulation of 3D polycrystalline microstructures. Part 1: Statistical characterization," *Acta Materialia*, Vol. 56, Issue 6, April 2008, pp. 1257-1273.

88   Groeber, M., Ghosh, S., Uchic, M.D., and Dimiduk, D.M., "A framework for automated analysis and simulation of 3D polycrystalline microstructures. Part 2: Synthetic structure generation," *Acta Materialia*, Vol. 56, Issue 6, April 2008, pp. 1274-1287.

89   MacSleyne, J.P., Simmons, J.P., and De Graef, M., "On the use of moment invariants for the automated analysis of 3D particle shapes", *Modeling and Simulation in Materials Science and Engineering*, Vol. 16, April 2008, 17 pages.

90   Lathi, B. P. (2004). *Linear Systems and Signals*: Oxford University Press.

91   Cha, S., "Comprehensive Survey on Distance/Similarity Measures between Probability Density Functions," *International Journal of Mathematical Models and Methods in Applied Sciences*, Vol. 1, Issue 4, December 2007, pp. 300-307.

92   Kailath, T., "The Divergence & Bhattacharyya Distance Measures in Signal Selection," *IEEE Transactions on Communication Technology*, Vol. 15, Issue 1, February 1967, pp. 52-60.

93   Thacker, N.A., Aherne, F.J, and Rockett, P.I., "The Bhattacharyya metric as an absolute similarity measure for frequency coded data," *Kybernetika*, Vol. 34, Issue 4, 1998, pp. 363-368.

94   Comaniciu, D., Ramesh, V., and Meer, P., "Kernel-based object tracking," *IEEE Transactions on Pattern Analysis and Machine Intelligence*, Vol. 25, Issue 5, May, 2003, pp. 564–577.

95   Riley, M.E., and Grandhi, RV., "Quantification of model-form and predictive uncertainty for multi-physics simulation," *Computers and Structures*, Vol. 89, Issues 11-12, June 2011, pp. 1206-1213.

96   Callahan, P.G. (2012) *Quantitative characterization and comparison of precipitate and grain shape in Ni-base superalloys using moment invariants* (Electronic Dissertation). (Publication No. 3532718)

97   Morris, J.W., "The influence of grain size on the mechanical properties of steel," in *The International Symposium on Ultrafine Grained Steels Proceedings*, Tokyo, 2001, p. 34.

98   Loughnane, G., Groeber, M., Uchic, M., Riley, M., Shah, M., Srinivasan, R., and Grandhi, R., "Quantifying the Effect of 3D Spatial Resolution on the Accuracy of Microstructural Distributions," *in 1st International Conference on 3D Materials Science Proceedings*, Seven Springs, PA, July 2012, pp. 49-59.

99   Loughnane, G., Groeber, M., Uchic, M., Shah, M., Srinivasan, R., Grandhi, R., "Modeling the effect of voxel resolution on the accuracy of phantom grain ensemble statistics," *Materials Characterization*, Vol. 90, April 2014, pp. 136-150.

100 Callister, W.D, and Rethwisch, D.G. (2011). *Fundamentals of Materials Science and Engineering: An Integrated Approach*: Wiley

101 Candes, E.J., Romberg, J., and Tao, T., "Robust uncertainty principles: Exact signal reconstruction from highly incomplete frequency information," *IEEE Transactions on Information Theory*, Vol. 52, Issue 2, 2006, pp. 489-509.

102 Candes, E.J., and Wakin, M.B., "An introduction to compressive sampling," *IEEE Signal Processing Magazine*, Vol. 25, Issue 2, 2008, pp. 21-30.

103 Fornasier, M., and Rauhut, H. (2011) *Compressive Sensing*: Springer.

104 Tucker, J.C., Chan, L.H., Rohrer, G.S., Groeber, M.A., and Rollett, A.D., "Comparison of grain size distributions in a Ni-based superalloy in three and two dimensions using Saltykov Method," *Scripta Materialia*, Vol. 66, Issue 8, April 2012, pp. 554-557.

105 Sosa, J.M., Huber, D.E., Welk, B., and Fraser, H.L., "Development and application of MIPAR: a novel software package for two- and three-dimensional microstructural characterization," *Integrating Materials and Manufacturing Innovation*, Vol. 3, Issue 10, April, 2014

106 Gundersen, H.J.G., Jensen, T.B., and Osterby, R., "Distribution of membrane thickness determined by lineal analysis," *Journal of Microscopy*, Vol. 113, Issue 1, May 1978, pp. 27-43.

107 Kriczky, D. A., Irwin, J., Reutzel, E. D., Michaleris, P., Nassar, A. B., Craig, J., "3D spatial resolution of thermal characteristics in directed energy deposition through optical thermal imaging," *Journal of Materials Processing Technology*, Vol. 221, July 2015, pp. 172-186.

108 Gockel, J.E. (2014) *Integrated Control of Solidification Microstructure and Melt Pool Dimensions in Additive Manufacturing of Ti-6A-4V* (Electronic Dissertation). Retrieved from http://repository.cmu.edu/dissertations/374.

109 Humbert, M., Moustahfid, H., Wagner, F., and Phillipe, M.J., "Evaluation of the High Temperature ß Texture of a Sample of TA6V from Individual Orientation Measurements of

Plates of the α Phase at Room Temperature," *Materials Science Forum*, Vol. 157, 1994, pp. 1225-1230.

110 Humbert, M., Wagner, F., Moustahfid, H., and Esling, C., "Determination of the Orientation of a Parent β Grain from the Orientations of the Inherited α Plates in the Phase Transformation from Body-Centered Cubic to Hexagonal Close Packed," *Journal of Applied Crystallography*, Vol. 28, 1995, pp. 571-576.

111 Glavicic, M.G., Kobryn, P.A., Bieler, T.R., and Semiatin, S.L., "A method to determine the orientation of the high-temperature beta phase from measured EBSD data for the low-temperature alpha phase in Ti-6Al-4V," *Materials Science and Engineering: A*, Vol. 346, 2003, pp. 50-59.

112 Glavicic, M.G., Kobryn, P.A., Bieler, T.R., and Semiatin, S.L., "An automated method to determine the orientation of the high-temperature beta phase from measured EBSD data for the low-temperature alpha-phase in Ti-6Al-4V," *Materials Science and Engineering: A*, Vol. 351, 2003, pp. 258-264.